Titre: Title:	Investigating the Al/Si mixed site occupancy in the β-AlFeSi phase
Auteurs: Authors:	Paul Lafaye, Minh Duc Vo, Javier Jofré, & Jean-Philippe Harvey
Date:	2023
Type:	Article de revue / Article
Référence: Citation:	Lafaye, P., Vo, M. D., Jofré, J., & Harvey, J.-P. (2023). Investigating the Al/Si mixed site occupancy in the β-AlFeSi phase. Physical Chemistry Chemical Physics, 25(29), 20015-20025. https://doi.org/10.1039/d3cp01940c

Physical Chemistry Chemical Physics

journal homepage: https://www.rsc.org/journals-books-databases/about-journals/pccp

Investigating the Al/Si Mixed Site Occupancy in the β-AlFeSi Phase

Paul Lafaye[a]*, Minh Duc Vo[a], Javier Jofre[a], Jean-Philippe Harvey[a]

[a] *CRCT- Polytechnique Montréal, Chem. Eng., Box 6079, Station Downtown, Montréal, Qc, Canada, H3C 3A7*

Abstract

This work investigates the mixed site occupancy of aluminium and silicon atoms in the β-AlFeSi phase. For this purpose, the six mixed Al/Si sites of the β-AlFeSi structure were considered independent and alternatively substituted by Al or Si, thus generating 64 ordered structures or *end-members*. The enthalpy of formation of each *end-member* was calculated by DFT. These calculations allowed us to derive the enthalpy of mixing of the solid solution at 0 K, over a wide range of chemical compositions, from the Al-Fe binary system to the Si-Fe binary system. In addition, the heat capacities of the solid solution were determined using a Debye model based on the calculation of the elastic constants and equation of state of each end-member. These heat capacity values were used along with the enthalpy of formation we calculated to determine the Gibbs free energy of all the *end-members* of the β-AlFeSi structure. Finally, the configurational entropy of mixing from the Compound Energy Formalism (CEF) for the configurational entropy of mixing was subsequently used to calculate the Si site occupation fractions on the Al sites of the β-AlFeSi structure, at 300 K and 938 K, the latter being the thermal decomposition temperature of this compound. These original site occupancy data were used to quantify the chemical ordering of the solid solution and to compare different sublattice (SL) model. We thus highlight that the SL model of the β-AlFeSi solution most commonly accepted in the literature generates considerable errors in its thermodynamic description, contrary to the model proposed in this paper, which is both simple and particularly accurate, consisting in merging the sites Al(1)-Al(6), the sites Al(2)-Al(3) as well as the sites Al(4)-Al(5).

Keywords: β-AlFeSi phase, crystal chemistry, DFT calculations, Heat capacity calculations, Thermodynamic modelling

1. Introduction

The energetics of condensed phases are of prime importance when exploring the thermodynamic behaviour of multicomponent metallic systems which are used to produce alloys. The energetic behaviour of a solid is largely defined by its internal structure which modulates the type, number, and strength of chemical interactions. This work is a contribution to a larger research project which consists in investigating the relevance of the

thermodynamic models (sublattice or SL models) used to describe the primary solidification phases of aluminium alloys *via* the Compound Energy Formalism (CEF) [1]. The design of a SL model should be, in principle, be based on the characterisation of the non-stoichiometry of the phase of interest, *i.e.*, substitutional disorder, interstitial disorder or the presence of vacancies. However, these data can be difficult to obtain experimentally. In the case of aluminium alloys, many primary solidification phases exhibit homogeneity ranges resulting from substitution between neighbouring elements in the periodic table. This is the case, for example, of the $Al_{13}(Fe,X)_4$ solid solutions that have been investigated in previous studies [2, 3], but also of the α-AlFeSi, β-AlFeSi, γ-AlFeSi and α-AlMnSi phases for which substitutions between Al and Si are responsible for their non-stoichiometry [4-12]. For these solid solutions, the similarity in electronic structure between the two elements involved in the substitution makes them almost impossible to distinguish using conventional X-ray diffraction techniques. Furthermore, these phases may have relatively restricted homogeneity ranges as it is the case for the ternary intermetallic phases of the Al-Fe-Si system [4-8], which further complicates the experimental characterisation of their crystal chemistry. In this context, it becomes challenging to understand the origin of the non-stoichiometry of these phases. For this reason, the construction of their SL model has often been based on purely practical considerations in the absence of thermodynamic evidence [13-15].

This is the case for the β-AlFeSi phase. Indeed, Romming *et al.* [4] noted the presence of six Al/Si mixed sites in the structure even though it was not possible to distinguish Si and Al atoms. As a result, the six Al/Si mixed sites of the structure were uniformly labelled as Al sites. This notation [4] is utilized throughout the paper. This phase has a particularly limited homogeneity range [4-8], which is why several authors have modelled it as a stoichiometric compound [13-15]. On the contrary, this work shows that it should be modelled as a solution since there is a significant substitutional disordering on the Al sites of the structure. In addition, we point out in this paper that the thermodynamics of this solution is peculiar and that the SL models available in the literature do not capture this behaviour. The inability of a given SL model to reflect the ordering of the solution is problematic since it imposes a configurational entropy of mixing that may be erroneous, leading to a poor description of the thermodynamic stability of the solution.

This work characterizes the crystal chemistry of the β-AlFeSi phase over a wide range of temperatures and compositions, mimicking the complete substitution on the crystal sites via 0K DFT simulations. To this end, we have calculated by DFT the enthalpies of formation of all ordered configurations corresponding to permutations between Al and Si on the Al sites of the β-AlFeSi structure which generated 64 distinct configurations. The Gibbs free energy functions of these 64 structures were then determined by calculating their isobaric heat capacities using a Debye model. At last, the CEF was used to calculate the Si site occupation factors (*sof*) on the Al sites of the β-AlFeSi structure at 300 K and 938 K (i.e., the decomposition temperature of the stoichiometric phase). This research deepens and completes the understanding of the thermodynamic behaviour of the β-AlFeSi primary

solidification phase allowing the construction of a reliable SL model resulting from the merging sites Al(1)-Al(6), sites Al(2)-Al(3) and sites Al(4)-Al(5).

2. Literature review

The Al-Fe-Si ternary system is composed of nearly a dozen of ternary phases. These phases, traditionally numbered from τ_1 to τ_{11}, are present throughout the whole ternary composition range. In the case of wrought aluminium alloys, the critical Al-Fe-Si phases are τ_5 and τ_6, also known as the α-AlFeSi and β-AlFeSi phases, respectively. The presence of the β-AlFeSi phase in the ternary Al-Fe-Si system was first established by Resenhain *et al.* [16] and was later confirmed by Dix and Heath [17] in an investigation in the Al-rich corner of the ternary system. The β-AlFeSi intermetallic forms plate-like precipitates that can favour the initiation of local cracks in the microstructure and can lead to surface defects in the alloy [18]. The transformation of this harmful phase to the less detrimental α-Al(Fe,Mn)Si phase by adding manganese is a critical process in manufacturing 6000 series aluminium alloys [18].

Invariant reactions of the Al-Fe-Si phase were evaluated by Krendelsburger *et al.* [8]; the reaction $L + \tau_2 + \tau_4 = \tau_6$ forming β-AlFeSi was measured to occur at 938 K. Pontevichi *et al.* [19] found a temperature of 940 K. At the same time, calculations performed by Du *et al.* [14] from their thermodynamic assessment of the Al-Fe-Si ternary system gave a temperature of 932 K. Stefaniay *et al.* [7] evaluated the composition range of the β-phase in a heat-treated alloy finding ranges of 15.3-15.9 at.% for Fe and 15.7-18.1 at.% for Si around 873 K. Krendelsburger *et al.* [8] found a composition range of 64.5-67.5 at.% for Al, 15.5-16.5 at.% for Fe and 17-19 at. % for Si.

Determining the crystal structure and composition of the β-AlFeSi phase was the focus of multiple studies [4, 20-29]. A consensus on the crystallography of the phase was delayed because of the conflicting reported structures. Indeed, monoclinic, tetragonal, and orthorhombic structures were all proposed. From X-ray diffraction experiments, Phragmen [20] first reported a monoclinic unit cell with lattice parameters a = 6.12, b = 6.12, c = 41.5 Å and β = 91°. From electron microscopy, Hoier *et al.* [23] also found a monoclinic unit cell with a = 6.18, b = 6.18, c = 20.8 Å and β = 91°. Following the work of Phragmen [20], Black [21] reported a 4/*m* Laue symmetry with cell parameters a = 6.18 and c = 42.5 Å. Black [21] proposed the formula $Al_9Fe_2Si_2$ (or the equivalent $Al_{4.5}FeSi$) corresponding to approximately 15.3 at.% Fe and 15.4 at.% Si. Panday and Schubert [22] also found a tetragonal cell but with parameters a = 6.07 and c = 9.5 Å. Kral [26] later found that the previous description of a tetragonal β-phase by Panday and Schubert was in fact the distinct δ-Al_5FeSi_2 phase. Carpenter and Le Page [24] described an orthorhombic B-centered cell with a = 6.18, b = 6.25 and c = 20.69 Å and proposed the formula Al_5Fe_2Si. Similarly, Zheng *et al.* [25] examined the crystal structure of an orthorhombic β-phase with space group *Cmcm* and proposed the formula Al_5FeSi. Studies on the polytypes of the β-phase structure were made by Becker *et al.* [27, 29] to reconcile the past studies on the phase. The acknowledged consensus structure

for the β-AlFeSi phase was proposed by Romming *et al.* [4] in a thorough investigation of the β-$Al_{4.5}$FeSi using both X-ray diffraction and electron microscopy. They found a monoclinic structure with space group *A*2/*a* (15) with cell dimensions $a = 6.161$, $b = 6.175$, $c = 20.813$ Å and $\beta = 90.42°$ [4]. It is important to note that the structure of the β-AlFeSi phase does belong to the monoclinic crystal system despite having a β angle very close to 90° and almost equal *a* and *b* lattice parameters. The structure is, therefore, very close to the tetragonal crystal systems. This peculiarity has led to disagreements in the literature about the crystallographic structure of the β-AlFeSi phase. Furthermore, in recognition of this specificity, Romming *et al.* [4] proposed the notation *A*2/*a* and not *C*2/*c*, thus allowing the β-AlFeSi structure to be described with a single *c*-axis, as is the case for orthorhombic/tetragonal structures. A total of 52 atoms are present in the unit cell, with 8 being iron atoms and the remaining 44 being a mix of aluminium and silicon atoms. The crystallography of the β-AlFeSi phase, as reported by Romming *et al.* [4], is presented in Table 1.

Table 1: Crystal structure of the β-AlFeSi phase according to Romming *et al.* [4].

Site	Wyckoff position	*x*	*y*	*z*
Fe (1)	8*f*	0.5024	0.2605	0.1367
Al (1)	8*f*	0.3583	0.6062	0.1863
Al (2)	8*f*	0.3387	-0.0884	0.0897
Al (3)	8*f*	0.1669	0.4167	0.0908
Al (4)	8*f*	0.4972	0.2666	0.0181
Al (5)	4*c*	0.5000	0.2500	0.2500
Al (6)	8*f*	0.1526	0.1000	0.1836

Calorimetric measurements for the heat of formation of ternary Al-Fe-Si phases were made by Vybornov *et al.* [30] and by Li and Legendre [31]. Vybornov *et al.* [30] indirectly determined the enthalpy of formation for the α-AlFeSi and β-AlFeSi phases by measuring the heats of dissolution of the pure elements and of the β-AlFeSi phases in an aluminium bath at 1373 K and found an enthalpy of formation at 298 K of -24.5 ± 2 kJ/mol for the latter. Li and Legendre [31, 32] determined the enthalpy of formation for many Al-Fe-Si ternary phases using the same indirect method as Vybornov *et al.* [30]. For the β-AlFeSi phase, they determined an enthalpy of formation at 298 K of -20.209 ± 1 kJ/mol. No information on the heat capacity of the β-AlFeSi phase was reported. Recently, Fang *et al.* [28] used first-principles calculations to evaluate the crystal chemistry and electronic structure of the β-AlFeSi phase. These authors have established that the formation of vacancies on the Fe or Al sites of the β-AlFeSi structure is very unfavourable from an energetic perspective. Similarly, their investigation showed that only Al and Si elements can substitute on the Al sites of the structure. Substitutions of Al or Si on the Fe sites, and reciprocally, the substitution of Fe on the Al sites of the structure being also very unfavourable. According

to Fang *et al.* [28], Si substitution occurs preferentially on sites Al(1)-Al(6) and then on sites Al(5), Al(2)-Al(3) and Al(4).

In early thermodynamic assessments of the system, the β-AlFeSi phase was considered as a stoichiometric compound. This is notably the case in an assessment included in the COST507 database for aluminium alloys [13]. Du *et al.* [14] reassessed the Al-Fe-Si system using their own experimental data together with literature data. Their description included a reoptimized β-AlFeSi phase with new parameters, but Du *et al.* [14] maintained the phase as a stoichiometric compound. Semi-stoichiometric descriptions started with the assessment by Liu and Chang [5]. They proposed the sublattice model $Al_{0.598}\,Fe_{0.152}\,Si_{0.10}\,(Al,\,Si)_{0.15}$ to describe more accurately the observed composition range along the Al-Si axis. This model was accepted in assessments of the Al-Fe-Si ternary by Eleno *et al.* [6], Chen *et al.* [33] and Zienert [34]. Although experimental data also suggest a small homogeneity range in iron, the semi-stoichiometric description of β-phase was found satisfactory in these assessments.

3. Methodology

3.1. DFT calculations

We performed DFT calculations using the VASP code [35, 36], utilizing the Perdew-Burke-Ernzerhof exchange-correlation function [37] in the generalized gradient approximation framework, with a 10×10×3 k-points grid and a cutoff energy of 600 eV. For the Al, Fe, and Si elements, we selected Projector augmented wave (PAW) pseudopotentials with 3, 8, and 4 valence electrons, respectively. To account for the magnetic nature of Fe, we conducted spin polarized calculations, relaxing both the lattice parameters and atomic positions until the Hellman-Feynman forces were below 1 meV/Å. We calculated the total energies of 64 *end-members* based on the distribution of Al and Si atoms on the six non-equivalent Al sites of the β-AlFeSi. The crystal site coordinates of the β-AlFeSi structure can be found in Table 1. The enthalpy of formation of the ordered compound was determined by calculating the difference between the compound's total energy and the sum of the pure element energies in their respective standard state (Al-*fcc*, Fe-*bcc*, Si-A*4*).

3.2. Debye model for the heat capacity calculations

The isobaric heat capacities were calculated from the Helmholtz free energy using a Debye approach within the Quasi-Harmonic Approximation (QHA) [38] for determining the vibrational contribution. The parametrization of the internal energy was performed by fitting the Birch-Murnaghan equation of state to DFT total energy data as a function of volume obtained using VASP [35, 36]. The Debye-Wang model [38] was used in its Slater form for the calculation of the Debye temperature. The elastic constants of the 64 *end-members* were calculated from the stress-strain tensor by imposing 55 finite distortions on the lattice, using the VASP code [35, 36]. The elastic

constant values are reported in Appendix. The electronic contribution to the free energy was taken as a function of the volume-dependent electronic DOS evaluated at the fermi level. In addition, no thermal vacancy nor explicit anharmonic contributions were considered. The results of the heat capacity calculations are presented in Appendix.

3.3. Thermodynamic modelling

The Gibbs free energy of a specific phase at a finite temperature can be determined from the 0 K DFT calculations of the formation enthalpies and isobaric heat capacities of all its *end-members* by means of the Compound Energy Formalism (CEF) [1]. Interactions within sublattices can be implemented *via* interaction parameters. Numerous studies have been conducted using the CEF, and the reader interested in further explanation is referred to our previous work using this methodology [39, 40].

4. Results and discussion

The formation enthalpies of the 64 *end-members* that we calculated in this work are reported in Table 2. These calculations allowed us to determine the enthalpy of mixing of the β-AlFeSi solid solution by considering as reference the perfectly ordered *end-members* corresponding to a complete occupation of sites Al(1) to Al(6) by Al on the one hand and by Si on the other hand. Therefore, the β-AlFeSi solid solution can be characterised in the whole composition range, from the Al-Fe binary system to the Si-Fe binary system, as shown in Figure 1.

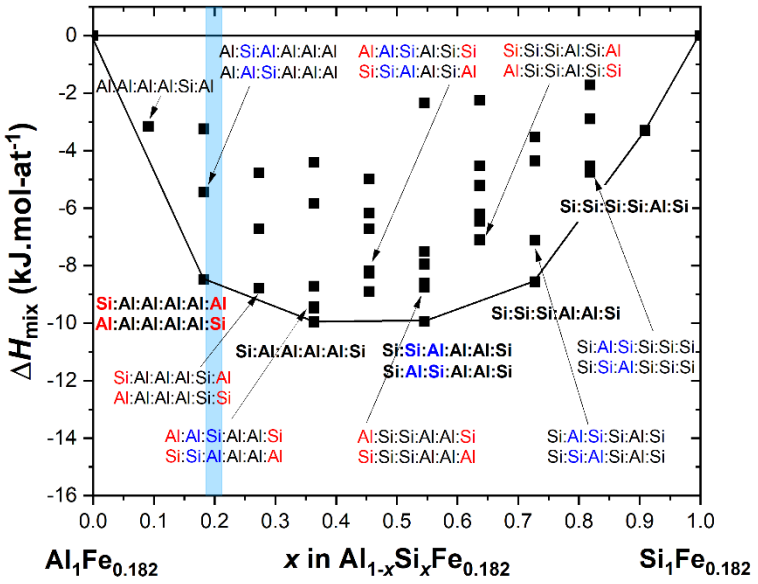

Figure 1: Mixing enthalpy of the β-AlFeSi solid solution calculated at 0 K (Refs: $Al_1Fe_{0.182}$ and $Si_1Fe_{0.182}$). The homogeneity range of the solid solution is highlighted by the blue band.

Table 2. DFT calculated total energy (E_{tot}) and enthalpy of formation (ΔH_f) of the β-AlFeSi solid solution *end-members*. Sites are taken from [4]. Reference Al (*fcc*), Fe (*bcc*) and Si (*A*4).

Site							E_{tot} (eV)	ΔH_f (kJ.mol-at^{-1})
Fe (1)	Al (1)	Al (2)	Al (3)	Al (4)	Al (5)	Al (6)		
Multiplicity								
8	8	8	8	8	4	8		
Fe	Al	Al	Al	Al	Al	Al	-241.159	-19.331
Fe	Al	Al	Al	Al	Si	Al	-248.358	-22.053
Fe	Al	Al	Al	Al	Al	Si	-256.727	-26.947
Fe	Al	Al	Al	Si	Al	Al	-253.909	-21.717
Fe	Al	Al	Si	Al	Al	Al	-255.096	-23.921
Fe	Al	Si	Al	Al	Al	Al	-255.097	-23.921
Fe	Si	Al	Al	Al	Al	Al	-256.727	-26.947
Fe	Al	Al	Al	Al	Si	Si	-262.394	-26.827
Fe	Al	Al	Al	Si	Si	Al	-260.230	-22.811
Fe	Al	Al	Si	Al	Si	Al	-261.284	-24.767
Fe	Al	Si	Al	Al	Si	Al	-261.285	-24.768
Fe	Si	Al	Al	Al	Si	Al	-262.394	-26.827
Fe	Al	Al	Al	Si	Al	Si	-268.281	-27.114
Fe	Al	Al	Si	Al	Al	Si	-268.526	-27.569
Fe	Al	Al	Si	Si	Al	Al	-265.537	-22.023
Fe	Al	Si	Al	Al	Al	Si	-268.249	-27.055
Fe	Al	Si	Al	Si	Al	Al	-265.537	-22.023
Fe	Al	Si	Si	Al	Al	Al	-266.308	-23.454
Fe	Si	Al	Al	Al	Al	Si	-268.540	-27.595
Fe	Si	Al	Al	Si	Al	Al	-267.860	-26.334
Fe	Si	Al	Si	Al	Al	Al	-268.249	-27.054
Fe	Si	Si	Al	Al	Al	Al	-268.527	-27.570
Fe	Al	Al	Al	Si	Si	Si	-273.077	-25.378

Fe	Al	Al	Si	Al	Si	Si	-273.458	-26.085
Fe	Al	Al	Si	Si	Si	Al	-271.352	-22.177
Fe	Al	Si	Al	Al	Si	Si	-273.114	-25.446
Fe	Al	Si	Al	Si	Si	Al	-271.350	-22.173
Fe	Al	Si	Si	Al	Si	Al	-271.994	-23.368
Fe	Si	Al	Al	Al	Si	Si	-272.281	-23.901
Fe	Si	Al	Al	Si	Si	Al	-273.076	-25.375
Fe	Si	Al	Si	Al	Si	Al	-273.113	-25.446
Fe	Si	Si	Al	Al	Si	Al	-273.459	-26.086
Fe	Al	Al	Si	Si	Al	Si	-278.450	-24.711
Fe	Al	Si	Al	Si	Al	Si	-278.218	-24.282
Fe	Al	Si	Si	Al	Al	Si	-278.803	-25.367
Fe	Al	Si	Si	Si	Al	Al	-275.433	-19.114
Fe	Si	Al	Al	Si	Al	Si	-278.886	-25.522
Fe	Si	Al	Si	Al	Al	Si	-279.525	-26.706
Fe	Si	Al	Si	Si	Al	Al	-278.218	-24.281
Fe	Si	Si	Al	Al	Al	Si	-279.524	-26.706
Fe	Si	Si	Al	Si	Al	Al	-278.448	-24.709
Fe	Si	Si	Si	Al	Al	Al	-278.803	-25.367
Fe	Al	Al	Si	Si	Si	Si	-283.007	-22.533
Fe	Al	Si	Al	Si	Si	Si	-282.480	-21.554
Fe	Al	Si	Si	Al	Si	Si	-283.495	-23.438
Fe	Al	Si	Si	Si	Si	Al	-280.879	-18.584
Fe	Si	Al	Al	Si	Si	Si	-282.113	-20.873
Fe	Si	Al	Si	Al	Si	Si	-283.147	-22.793
Fe	Si	Al	Si	Si	Si	Al	-282.480	-21.554
Fe	Si	Si	Al	Al	Si	Si	-283.148	-22.793
Fe	Si	Si	Al	Si	Si	Al	-283.008	-22.534
Fe	Si	Si	Si	Al	Si	Al	-283.495	-23.438
Fe	Al	Si	Si	Si	Al	Si	-287.519	-20.270
Fe	Si	Al	Si	Si	Al	Si	-289.010	-23.036
Fe	Si	Si	Al	Si	Al	Si	-289.010	-23.036
Fe	Si	Si	Si	Al	Al	Si	-289.784	-24.472
Fe	Si	Si	Si	Si	Al	Al	-287.066	-19.428
Fe	Al	Si	Si	Si	Si	Si	-292.233	-18.380
Fe	Si	Al	Si	Si	Si	Si	-293.110	-20.008
Fe	Si	Si	Al	Si	Si	Si	-293.110	-20.008
Fe	Si	Si	Si	Al	Si	Si	-293.232	-20.235
Fe	Si	Si	Si	Si	Si	Al	-291.597	-17.200
Fe	Si	Si	Si	Si	Al	Si	-297.952	-18.356
Fe	Si	Si	Si	Si	Si	Si	-301.676	-14.631

Firstly, it should be noted that Figure 1 and Table 2 reveal a remarkable behaviour of the solid solution concerning the exact thermodynamic equivalence between several distinct crystal sites. Indeed, our DFT calculations have shown that each pair of *end-members* obtained by exchanging Al and Si elements on sites Al(1) and Al(6) only, have the same energy. For example, the *end-members* Si:Al:Al:Al:Al:Al and Al:Al:Al:Al:Al:Si both have an enthalpy of formation of exactly −26.947 kJ/mol-at^{-1}. All *end-members* meeting these characteristics have been highlighted in red in Figure 1. The same behaviour is observed between sites Al(2) and Al(3) of the structure, as shown in blue in Figure 1. This particularity is quite interesting since it allows us, without further calculations, to define the first SL of the β-AlFeSi structure by merging the crystal sites Al(1) and Al(6) in a single SL, and crystal sites Al(2) and Al(3) on a second SL. This thermodynamic equivalence between sites Al(1) and Al(6) on the one

hand and between sites Al(2) and Al(3) on the other hand has also been reported by Fang *et. al.* [28]. In addition, it should be noted that the calculations reported in Figure 1 show that Si substitution on Al sites appears to be sequential, with a preferential occupation on sites Al(1)-Al(6), then on sites Al(2)-Al(3). In contrast, the sites Al(4) and Al(5) are the least favourable for Si substitution. It is important to note at this step that Fang *et. al.* [28] stated that the preferred sites for Si substitutions are the sites Al(1)-Al(6), then the site Al(5), Al(2)-Al(3) and Al(4) which is different from our results. This apparent contradiction originates in the chemical composition range investigated. Indeed, Fang *et. al.* calculations [28] were performed in the Si-poor region (x less than 0.18 in $Al_{1-x}Si_xFe_{0.182}$) which is outside the homogeneity range of the β-AlFeSi phase. In this region, our calculations show that the Al(1)-Al(6) sites are the most favourable for Si substitution since the *end-members* Al:Al:Al:Al:Al:Si and Si:Al:Al:Al:Al:Al constitute the *ground-state* shown in Figure 1. One should also note that the *end-member* Al:Al:Al:Al:Si:Al at composition x = 0.09 (in $Al_{1-x}Si_xFe_{0.182}$) is the closest to the *ground-state* in this region, corresponding to Si substitution on site Al(5). The following *end-members*, listed in order of stability, are Al:Al:Si:Al:Al:Al and Al:Si:Al:Al:Al:Al at composition x = 0.18 (in $Al_{1-x}Si_xFe_{0.182}$) reflecting the substitution of Si on sites Al(2)-Al(3) and then the *end-member* Al:Al:Al:Si:Al:Al at the same composition. If we restrict our analysis to the calculations we performed in this Si-poor region (x less than 0.14), we thus obtain the same substitution sequence as the one given by Fang *et. al.* [28]. From the analysis of our calculations reported in Figure 1, we should therefore expect to find site occupancy values in agreement with this sequence in the Si-poor region. Our calculations, on the other hand, provide a characterisation of the substitutions over a much wider range of chemical compositions.

From the integration of the DFT and heat capacity calculations of the solid solution *end-members* into a CEF model, the Si site occupation factors (*sof*) on the Al sites of the β-AlFeSi solid solution was computed at 300 K and 938 K, as shown in Figure 2 and Figure 3, respectively.

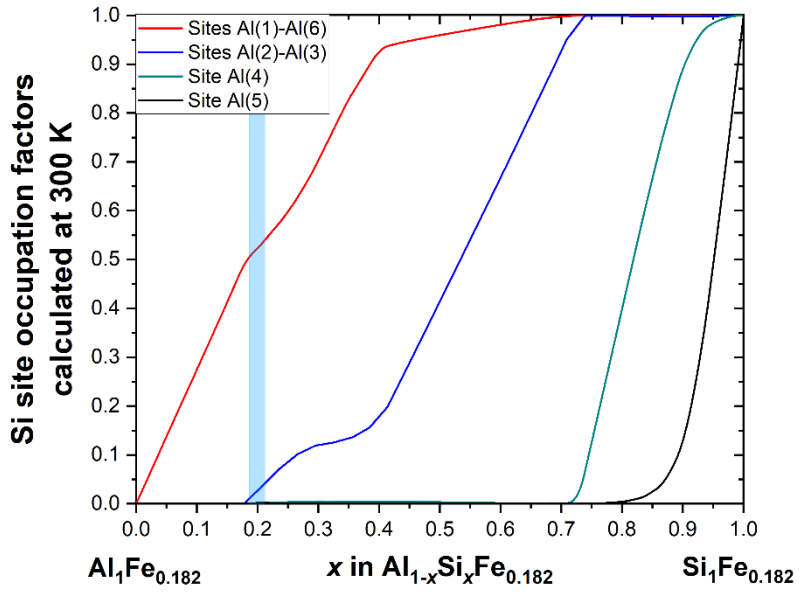

Figure 2: Si site occupation factors in the ß-AlFeSi solid solution, calculated at 300 K. The homogeneity range of the solid solution is highlighted by the blue band.

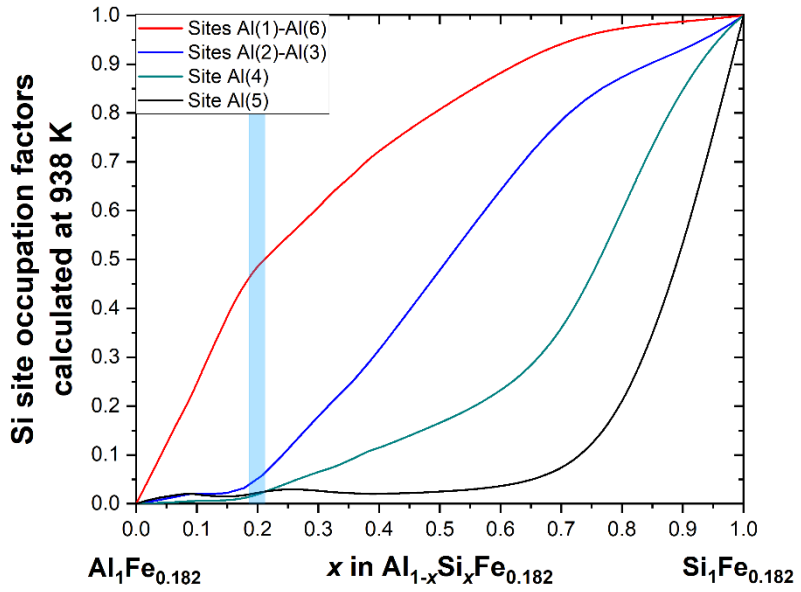

Figure 3: Si site occupation factors in the ß-AlFeSi solid solution, calculated at 938 K. The homogeneity range of the solid solution is highlighted by the blue band.

Figure 2 shows that the chemical ordering of the solid solution is strong at low temperatures. Indeed, the sites Al(4) and Al(5) do not accept mixing in the vicinity of the homogeneity range of the solution and the sites Al(2)-Al(3) only accept marginal Si substitution. Furthermore, it appears that the sites Al(1)-Al(6) and Al(2)-Al(3) show significant differences in Si *sof* at low Si contents (*x* less than 0.5 in $Al_{1-x}Si_xFe_{0.182}$). Only sites Al(4) and Al(5) show comparable occupancy values throughout the chemical composition range studied. However, at higher temperatures, the ordering of the solid solution is attenuated. In fact, all crystal sites in the structure are partially substituted by Si, although the preferential occupation on sites Al(1)-Al(6) remains substantial. This is certainly the case near the homogeneity domain of the β-AlFeSi structure presenting *sof* of sites Al(1)-Al(6) significantly higher than those of any other crystal sites. It is particularly interesting to note that at very low Si content (*x* less than 0.1 in $Al_{1-x}Si_xFe_{0.182}$), the sequence in which Si substitutes for Al is exactly the sequence reported by Fang *et. al.* [28]. Therefore, our results agree with those of Fang *et al.* since this is precisely the chemical composition range examined by these authors. Based on these calculations, the ordering of the solid solution was quantified by calculating its configurational entropy of mixing. These calculations are shown in Figure 4.

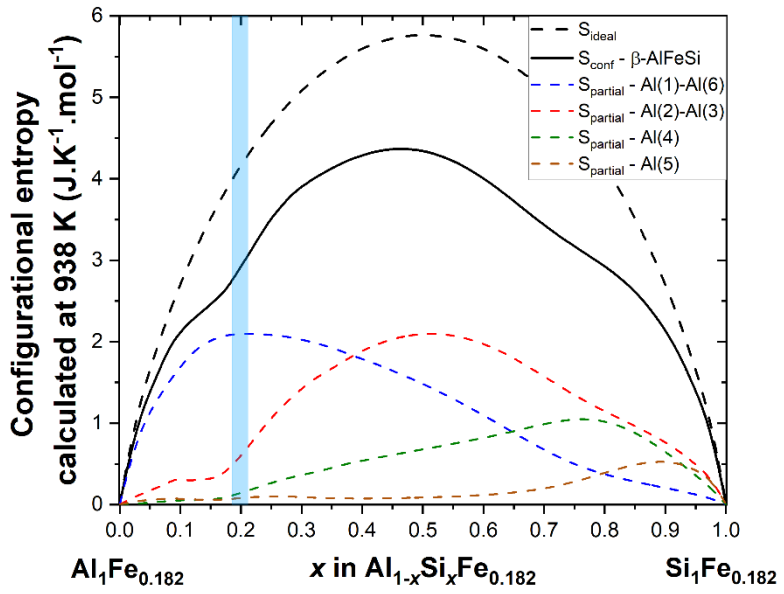

Figure 4: Configurational entropy of the β-AlFeSi solid solution calculated at 938 K compared to the configurational entropy of an ideal solution. The contribution of each crystal sites to the total configurational entropy of the solid solution is represented by the coloured dashed line.

This figure shows the total mixing entropy of the solution, as well as the individual contribution of each crystal site. One can also observe that the ordering level of the solid solution is relatively low at 938 K, although it seems inaccurate to consider the solution as purely ideal. It is interesting to note that the configurational entropy of the β-AlFeSi solid solution is alternatively dominated by the contribution of sites Al(1)-Al(6) for values of *x* lower than 0.38 (in $Al_{1-x}Si_xFe_{0.182}$) and by the contribution of sites Al(2)-Al(3) for values of *x* larger than 0.38. Also note that for values of *x* greater than 0.8 the contribution of sites Al(4) and Al(5) is substantial. The observation that the configurational entropy contribution of both sites Al(4) and Al(5) is significant in the same composition range

(x greater than 0.8 in $Al_{1-x}Si_xFe_{0.182}$) allows to simplify the SL model of the solution by merging these sites into a single SL. It should be noted that this finding is a consequence of the *sof* values calculated in Figure 2 and Figure 3, showing that both sites Al(4) and Al(5) have comparable occupancy values throughout the temperature range investigated. Figure 4 also shows that any further simplification would not be compatible with the thermodynamics of the solid solution. Indeed, the sites Al(1)-Al(6) cannot be combined with any other crystal site. This is because their contribution to the configurational entropy is significantly different from those of any other crystal site in the vicinity of the solid solution homogeneity range. Similarly, sites Al(2)-Al(3) cannot be merged with sites Al(4) and Al(5) since their contributions to the configurational entropy of the solution are quite different in the vicinity of x = 0.5 in $Al_{1-x}Si_xFe_{0.182}$. The simplest possible SL model is, therefore, a 3SL model, with one SL for sites Al(1) and Al(6), one SL for sites Al(2) and Al(3) and one SL for sites Al(4) and Al(5).

This 3-SL model drastically simplifies the solid solution model since it can be described with only 8 *end-members* in the Al-Fe-Si ternary system instead of the 64 *end-members* initially considered. The *ground-state* of the β-AlFeSi solid solution described with this 3-SL model from our DFT calculations only (orange curve) is plotted in Figure 5 and compared to the exact *ground-state* of the solution (black dashed curve).

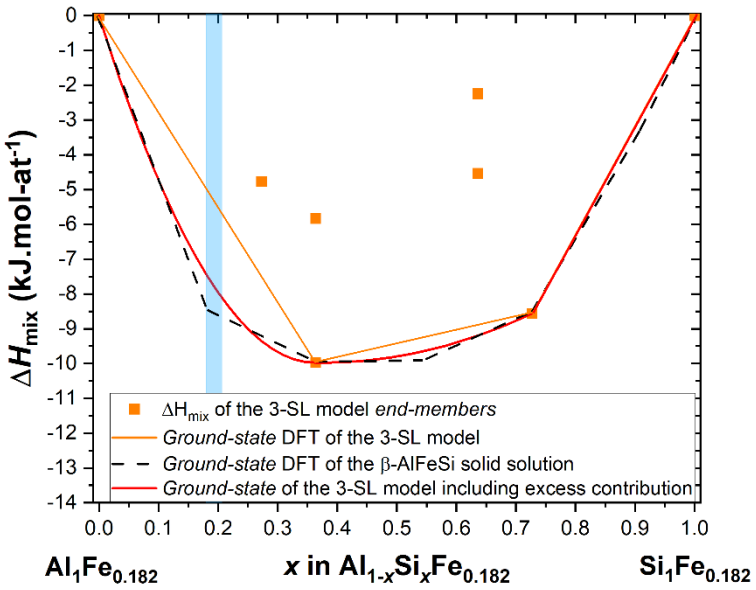

Figure 5: Ground-state of the β-AlFeSi solid solution based on the 3-SL model (orange curve) obtained from the 0 K DFT calculated mixing enthalpies of the 3-SL end-members (orange square), compared to the exact ground-state of the β-AlFeSi solid solution (black dashed curve). The red curve represents the ground-state of the β-AlFeSi solid solution including excess enthalpy contributions.

It should be noted that the 3-SL model allows reproducing the sequence of substitution Al(1)-Al(6), Al(2)-Al(3) and then Al(4)-Al(5) that we have calculated over a wide range of chemical compositions (x greater than 0.14 in $Al_{1-x}Si_xFe_{0.182}$ at 938 K). On the other hand, the existence of a single SL for both sites Al(4) and Al(5) prohibits the possibility of the substitution sequence that our calculations and those of Fang *et. al.* [28] have shown for low Si content. Furthermore, we note that the use of this 3-SL model induces a deviation of the thermodynamic

stability of the solution particularly pronounced for low Si concentrations (around $x = 0.2$ in $Al_{1-x}Si_xFe_{0.182}$). The implementation of the 3-SL model must therefore be accompanied by interaction parameters, as shown in Figure 5 (red curve). These interaction parameters were obtained by fitting the DFT-calculated ground-state of the solution shown as a dashed line in Figure 5. This is a novel and more accurate way of addressing the interaction parameters in the Calphad method. Indeed, the use of interaction parameters often meets the need to reproduce phase equilibria data [39, 40] whereas we show in this study that they should also be regarded as a tool allowing to correctly describe the thermodynamic behaviour of solid solution when simplified SL models are used.

The Gibbs free energy of all the 3-SL *end-members* of the β-AlFeSi solid solution as well as the interaction parameters used are reported in Table 3. Note that the Gibbs energy functions have been obtained directly from our calculations and do not result from fitting.

Table 3. Gibbs free energy of the β-AlFeSi solid solution *end-members* according to the 3-SL model developed in this study. Sites are taken from [4]. Reference Al (*fcc*), Fe (*bcc*) and Si (*A*4).

Sites / SL				Parameters (J/mol-at.)
Fe (1)	SL 1	SL 2	SL 3	
Multiplicity				
8	16	16	12	
Fe	Al	Al	Al	$G = -2.8837\times10^4 + 1.4336\times10^2\,T - 2.422\times10^1\,T\ln(T) - 1.6965\times10^{-3}\,T^2 - 1.870\times10^{-8}\,T^3 + 2.5405\times10^5\,T^{-1} + 7.252\times10^1\,T^{0.5} - 5.840\times10^6\,T^{-2}$
Fe	Al	Al	Si	$G = -3.2434\times10^4 + 1.4414\times10^2\,T - 2.421\times10^1\,T\ln(T) - 1.4895\times10^{-3}\,T^2 - 3.077\times10^{-8}\,T^3 + 2.7425\times10^5\,T^{-1} + 7.552\times10^1\,T^{0.5} - 6.565\times10^6\,T^{-2}$
Fe	Al	Si	Al	$G = -3.3089\times10^4 + 1.4428\times10^2\,T - 2.422\times10^1\,T\ln(T) - 1.3720\times10^{-3}\,T^2 - 5.243\times10^{-8}\,T^3 + 2.7725\times10^5\,T^{-1} + 7.592\times10^1\,T^{0.5} - 6.698\times10^6\,T^{-2}$
Fe	Si	Al	Al	$G = -3.7312\times10^4 + 1.4370\times10^2\,T - 2.412\times10^1\,T\ln(T) - 1.5535\times10^{-3}\,T^2 - 3.033\times10^{-8}\,T^3 + 2.8395\times10^5\,T^{-1} + 8.284\times10^1\,T^{0.5} - 6.930\times10^6\,T^{-2}$
Fe	Al	Si	Si	$G = -2.8439\times10^4 + 1.4211\times10^2\,T - 2.393\times10^1\,T\ln(T) - 1.8980\times10^{-3}\,T^2 - 4.275\times10^{-8}\,T^3 + 2.8945\times10^5\,T^{-1} + 9.840\times10^1\,T^{0.5} - 7.147\times10^6\,T^{-2}$
Fe	Si	Al	Si	$G = -3.0558\times10^4 + 1.4478\times10^2\,T - 2.424\times10^1\,T\ln(T) - 1.7255\times10^{-3}\,T^2 - 4.087\times10^{-8}\,T^3 + 2.8275\times10^5\,T^{-1} + 7.384\times10^1\,T^{0.5} - 6.887\times10^6\,T^{-2}$
Fe	Si	Si	Al	$G = -3.4164\times10^4 + 1.4615\times10^2\,T - 2.434\times10^1\,T\ln(T) - 1.5595\times10^{-3}\,T^2 - 4.493\times10^{-8}\,T^3 + 2.9245\times10^5\,T^{-1} + 6.672\times10^1\,T^{0.5} - 7.237\times10^6\,T^{-2}$
Fe	Si	Si	Si	$G = -2.4185\times10^4 + 1.4792\times10^2\,T - 2.457\times10^1\,T\ln(T) - 1.5675\times10^{-3}\,T^2 - 5.867\times10^{-8}\,T^3 + 2.8275\times10^5\,T^{-1} + 4.884\times10^1\,T^{0.5} - 6.867\times10^6\,T^{-2}$
				$L(Fe : Al,Si : Al : Al) = -624000$
				$L(Fe : Si : Al,Si : Al) = -78000$

The configurational entropy of mixing from our 3SL model has been plotted in Figure 6, using the heat capacities calculated in this study or obtained from the Kopp-Neumann Approximation (KNA) [39]. Figure 6 also includes the comparison with the exact configurational entropy of the solid solution, the ideal entropy of mixing and the configurational entropy of mixing from the SL model most commonly used in the literature.

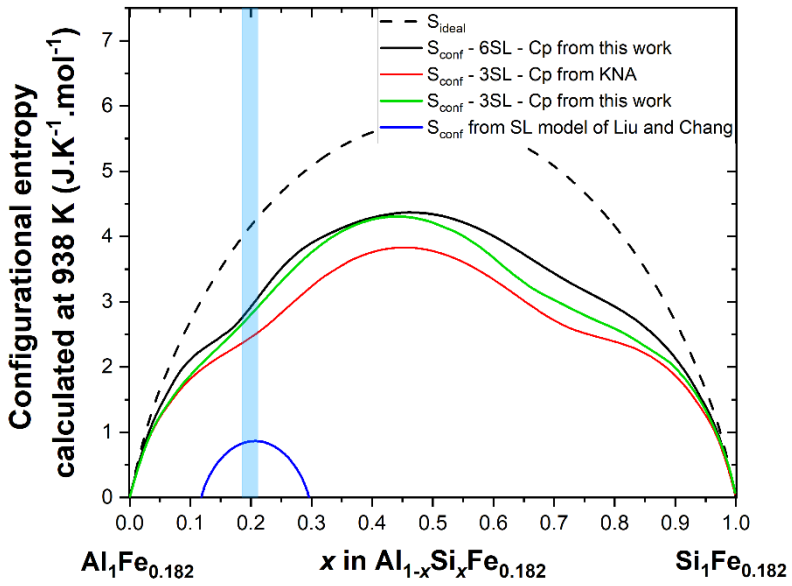

Figure 6: Configurational entropy at 938 K of the β-AlFeSi solid solution compared to the configurational entropy derived from the 3- SL models suggested in this study, and the SL model proposed by Liu and Chang [5] for the β-AlFeSi solid solution. The configurational entropy of an ideal solution is represented by the black dashed curve.

We note that the configurational entropy of mixing resulting from our 3-SL model is in good general agreement with the configurational entropy of the solution, in the vicinity of its homogeneity range but also beyond. Thus, the entire thermodynamics of the solution is correctly described by using this model. On the other hand, it is particularly striking to note that the most accepted SL model is not suitable for describing the solution. Indeed, this model only allows the solid solution to be described in a particularly restricted chemical composition range, centred on its stability domain. For this reason, this SL model has been labelled in this study as quasi-stoichiometric. More importantly, Figure 6 shows that this model leads to a large underestimation of the thermodynamic stability of the solid solution in the vicinity of its homogeneity domain. This poor thermodynamic estimation is problematic as it can be the source of significant errors affecting all phases in equilibrium with the solid solution. This highlights the importance of the choice of the SL model in the description of solid solutions, which should not be based on phase equilibria data alone but on the crystal chemistry of the solution. Finally, it is interesting to note the similarity of the configurational mixing entropies from the 3-SL model using the calculated heat capacities or obtained from KNA. This is because only the energy differences between the solution *end-members* contribute to the occupation of the crystal sites. Since the heat capacities obtained from KNA depend only on the chemical composition, the energy differences between *end-members* of the same composition remain identical to what we have calculated by DFT at 0 K. Note also that the heat capacities of the 64 *end-members* of the solid solution we calculated are very close, leading to almost constant energy differences between *end-members* as a function of temperature. For this reason, the use of KNA in the characterisation of the crystal chemistry of this solid solution can be considered acceptable. However, significant differences between calculated and KNA heat capacities can occur as reported in Appendix. It should also be noted that the use of KNA can lead

to unrealistic thermodynamic behaviour as presented in the Appendix. Indeed, the β-AlFeSi solid solution has been studied up to 938 K, which is higher than 933 K, the melting temperature of pure aluminium. For this reason, the KNA heat capacities of the solution *end-members* depict this melting of pure aluminium particularly at high Al content. As a result, even if the use of heat capacities obtained by KNA is not contraindicated for the characterisation of the crystal chemistry of the solution, we still recommend to calculate the heat capacities of all of the solid solution *end-members*.

5. Conclusion

In this paper, the β-AlFeSi solid solution has been studied in order to propose a SL model that is both simple to use (*i.e.*, generating a limited number of *end-members*) but robust in accurately modelling its thermodynamic behaviour. To this end, we calculated the Si site occupancy factors for the six Al sites of the β-AlFeSi structure at 300 K and 938 K (decomposition temperature of the solution) from the DFT calculation of the enthalpies of formation of the 64 *end-members* of the solution, as well as the calculation of their isobaric heat capacities. These new site occupancy data allowed us to design an optimal SL model whose configurational entropy at 938 K was compared to the exact configurational entropy of the β-AlFeSi structure as well as the one obtained by the most used SL model in the literature. We were able to show that our model describes the solid solution thermodynamics with a considerably improved accuracy compared to the literature model. Furthermore, our model allows a good description of the solution thermodynamics in the whole Al-Fe-Si ternary system, in contrast to the literature model. In addition, we have shown in this paper that the use of excess parameters for solid solution modelling should be reconsidered to include the description of the solution thermodynamics and not only the phase equilibrium data. Finally, it should be noted that our model is simple to use since only 8 *end-members* are required to describe the solution in the Al-Fe-Si ternary system instead of the 64 *end-members* initially considered.

Author Contributions

Paul Lafaye: Conceptualization, Investigation, Formal analysis, Writing-Original draft

Minh Duc Vo: Investigation, Formal analysis, Writing-Original draft

Javier Jofre: Investigation, Formal analysis, Writing-Original draft

Jean-Philippe Harvey: Supervision, Validation, Writing-Original draft

Conflicts of Interest

There are no conflicts to declare.

Acknowledgement

- This work was financially supported by the Professor Harvey Discovery Grant (RGPIN-2017-06168) (NSERC).
- Funding support was obtained through the Alliance Grant (ALLRP 560998 - 20).
- Compute Quebec and Compute Canada are thanked for supplying the intensive calculation tools.

References

[1] M. Hillert, The compound energy formalism, Journal of Alloys and Compounds 320(2) (2001) 161-176.
[2] P. Lafaye, K. Oishi, M. Bourdon, J.-P. Harvey, Crystal chemistry and thermodynamic modelling of the Al13 (Fe, TM) 4 solid solutions (TM= Co, Cr, Ni, Pt), Journal of Alloys and Compounds 920 (2022) 165779.
[3] P. Lafaye, K. Oishi, J.-P. Harvey, A comprehensive study on the thermodynamics of the Al13Fe4 solid solution in the Al-Fe-Mn ternary system, Journal of Alloys and Compounds 994 (2023) 169054.
[4] C. Rømming, V. Hansen, J. Gjønnes, Crystal structure of β-Al4. 5FeSi, Acta Crystallographica Section B: Structural Science 50(3) (1994) 307-312.
[5] Z.-K. Liu, Y.A. Chang, Thermodynamic assessment of the Al-Fe-Si system, Metallurgical and Materials Transactions A 30(4) (1999) 1081-1095.
[6] L. Eleno, J. Vezelý, B. Sundman, M. Cieslar, J. Lacaze, Assessment of the Al corner of the ternary Al–Fe–Si system, Materials Science Forum, Trans Tech Publ, 2010, pp. 523-528.
[7] V. Stefaniay, A. Griger, T. Turmezey, Intermetallic phases in the aluminium-side corner of the AlFeSi-alloy system, Journal of Materials science 22(2) (1987) 539-546.
[8] N. Krendelsberger, F. Weitzer, J.C. Schuster, On the reaction scheme and liquidus surface in the ternary system Al-Fe-Si, Metallurgical and materials transactions A 38 (2007) 1681-1691.
[9] M. Cooper, K. Robinson, The crystal structure of the ternary alloy α (AlMnSi), Acta Crystallographica 20(5) (1966) 614-617.
[10] M. Cooper, The crystal structure of the ternary alloy α (AlFeSi), Acta Crystallographica 23(6) (1967) 1106-1107.
[11] K. Sugiyama, N. Kaji, K. Hiraga, Re-refinement of α-(AlMnSi), Acta Crystallographica Section C: Crystal Structure Communications 54(4) (1998) 445-447.
[12] J. Roger, F. Bosselet, J. Viala, X-rays structural analysis and thermal stability studies of the ternary compound α-AlFeSi, Journal of Solid State Chemistry 184(5) (2011) 1120-1128.
[13] I. Ansara, A. Dinsdale, M. Rand, COST 507, Thermochemical database for light metal alloys 2 (1998) 75-78.
[14] Y. Du, J.C. Schuster, Z.-K. Liu, R. Hu, P. Nash, W. Sun, W. Zhang, J. Wang, L. Zhang, C. Tang, A thermodynamic description of the Al–Fe–Si system over the whole composition and temperature ranges via a hybrid approach of CALPHAD and key experiments, Intermetallics 16(4) (2008) 554-570.
[15] E. Balitchev, T. Jantzen, I. Hurtado, D. Neuschütz, Thermodynamic assessment of the quaternary system Al–Fe–Mn–Si in the Al-rich corner, Calphad 27(3) (2003) 275-278.
[16] W. Rosenhain, S.L. Archbutt, D. Hanson, Summary of the Eleventh Report to the Alloys Research Committee: On Some Alloys of Aluminium.(Light Alloys), Proceedings of the Institution of Mechanical Engineers 101(1) (1921) 699-771.
[17] E. Dix, A. Heath, Equilibrium relations in aluminum-silicon and aluminum-iron-silicon alloys of high purity, Trans. AIME 78 (1928) 164-194.
[18] N. Kuijpers, F. Vermolen, C. Vuik, P. Koenis, K. Nilsen, S. Van Der Zwaag, The dependence of the β-AlFeSi to α-Al (FeMn) Si transformation kinetics in Al–Mg–Si alloys on the alloying elements, Materials Science and Engineering: A 394(1-2) (2005) 9-19.
[19] S. Pontevichi, F. Bosselet, M. Peronnet, J. Viala, Thermostability of the beta-Al5FeSi phase in the ternary system Al-Fe-Si, Journal de Physique IV 113 (2004) 81-84.
[20] G. Phragmen, On the phases occurring in alloys of aluminium with copper, magnesium, manganese, iron, and silicon, Journal of the Institute of Metals 77(6) (1950) 489-551.
[21] P. Black, XLIX. Brillouin Zones of some intermetallic compounds, The London, Edinburgh, and Dublin Philosophical Magazine and Journal of Science 46(375) (1955) 401-409.
[22] P. Panday, K. Schubert, Strukturuntersuchungen in einigen Mischungen T-B3-B4 (T = Mn, Fe, Co, Ir, Ni, Pd; B3 = Al, Ga, Tl; B4 = Si, Ge), Journal of the Less Common Metals 18(3) (1969) 175-202.
[23] R. Hoier, ALFESI-PARTICLES IN AN AL-MG-SI-FE ALLOY, (1977).
[24] G. Carpenter, Y. Le Page, Revised cell data for the β-FeSiAl phase in aluminum alloys, Scripta metallurgica et materialia 28(6) (1993) 733-736.
[25] J. Zheng, R. Vincent, J. Steeds, Crystal structure of an orthorhombic phase in β-(Al-Fe-Si) precipitates determined by convergent-beam electron diffraction, Philosophical Magazine A 80(2) (2000) 493-500.
[26] M. Kral, A crystallographic identification of intermetallic phases in Al–Si alloys, Materials Letters 59(18) (2005) 2271-2276.

[27] H. Becker, T. Bergh, P.E. Vullum, A. Leineweber, Y. Li, β-and δ-Al-Fe-Si intermetallic phase, their intergrowth and polytype formation, Journal of Alloys and Compounds 780 (2019) 917-929.
[28] C. Fang, Z. Que, Z. Fan, Crystal chemistry and electronic structure of the β-AlFeSi phase from first-principles, Journal of Solid State Chemistry 299 (2021) 122199.
[29] H. Becker, N. Bulut, J. Kortus, A. Leineweber, β-Al4. 5FeSi: Hierarchical crystal and defect structure: Reconciling experimental and theoretical evidence including the influence of Al vs. Si ordering on the crystal structure, Journal of Alloys and Compounds 911 (2022) 165015.
[30] M. Vybornov, P. Rogl, F. Sommer, On the thermodynamic stability and solid solution behavior of the phases τ5-Fe2Al7. 4Si and τ6-Fe2Al9Si2, Journal of alloys and compounds 247(1-2) (1997) 154-157.
[31] Y. Li, P. Ochin, A. Quivy, P. Telolahy, B. Legendre, Enthalpy of formation of Al–Fe–Si alloys (τ5, τ10, τ1, τ9), Journal of Alloys and Compounds 298(1-2) (2000) 198-202.
[32] Y. Li, B. Legendre, Enthalpy of formation of Al–Fe–Si alloys II (τ6, τ2, τ3, τ8, τ4), Journal of Alloys and Compounds 302(1-2) (2000) 187-191.
[33] H.-l. Chen, C. Qing, D. Yong, J. Bratberg, A. ENGSTRÖM, Update of Al-Fe-Si, Al-Mn-Si and Al-Fe-Mn-Si thermodynamic descriptions, Transactions of Nonferrous Metals Society of China 24(7) (2014) 2041-2053.
[34] T. Zienert, Predicting heat capacity and experimental investigations in the Al-Fe and Al-Fe-Si systems as part of the CALPHAD-type assessment of the Al-Fe-Mg-Si system, (2018).
[35] G. Kresse, J. Furthmüller, Efficient iterative schemes for ab initio total-energy calculations using a plane-wave basis set, Physical review B 54(16) (1996) 11169.
[36] G. Kresse, D. Joubert, From ultrasoft pseudopotentials to the projector augmented-wave method, Physical review b 59(3) (1999) 1758.
[37] J.P. Perdew, K. Burke, M. Ernzerhof, Generalized gradient approximation made simple, Physical review letters 77(18) (1996) 3865.
[38] Y. Wang, Z.-K. Liu, L.-Q. Chen, Thermodynamic properties of Al, Ni, NiAl, and Ni3Al from first-principles calculations, Acta Materialia 52(9) (2004) 2665-2671.
[39] P. Lafaye, Développement d'outils de modélisation thermodynamique pour la prédiction de l'état métallurgique d'alliages à base zirconium, Université Paris-Est, 2017.
[40] P. Lafaye, C. Toffolon-Masclet, J.-C. Crivello, J.-M. Joubert, Experimental study, first-principles calculation and thermodynamic modelling of the Cr–Fe–Nb–Sn–Zr quinary system for application as cladding materials in nuclear reactors, Journal of Nuclear Materials 544 (2021) 152692.

Appendix

Isobaric heat capacities (Cp) of the β-AlFeSi solid solution *end-members*. Reference Al (*fcc*), Fe (*bcc*) and Si (*A*4).

Site							Heat capacity, Cp (J/K.mol-at.)					
Fe (1)	Al (1)	Al (2)	Al (3)	Al (4)	Al (5)	Al (6)						
Multiplicity												
8	8	8	8	8	4	8	10^{1}	10^{-3} T	10^{5} T^{-2}	10^{-7} T^{2}	10^{1} $T^{-0.5}$	10^{7} T^{-3}
Fe	Al	Al	Al	Al	Al	Al	2.422	3.393	-5.081	1.122	1.813	3.504
Fe	Al	Al	Al	Al	Si	Al	2.416	3.095	-5.281	1.529	1.950	3.715
Fe	Al	Al	Al	Al	Al	Si	2.418	2.854	-5.470	1.656	1.938	3.927
Fe	Al	Al	Al	Si	Al	Al	2.424	3.230	-5.358	2.200	1.823	3.804
Fe	Al	Al	Si	Al	Al	Al	2.429	3.268	-5.352	2.612	1.703	3.788
Fe	Al	Si	Al	Al	Al	Al	2.401	3.359	-5.508	1.854	2.289	3.978
Fe	Si	Al	Al	Al	Al	Al	2.395	3.129	-5.576	1.669	2.408	4.051
Fe	Al	Al	Al	Al	Si	Si	2.400	3.250	-5.696	2.260	2.337	4.188
Fe	Al	Al	Al	Si	Si	Al	2.421	2.979	-5.485	1.846	1.888	3.939
Fe	Al	Al	Si	Al	Si	Al	2.448	3.212	-5.393	2.998	1.353	3.828
Fe	Al	Si	Al	Al	Si	Al	2.432	3.304	-5.458	2.578	1.663	3.898
Fe	Si	Al	Al	Al	Si	Al	2.411	3.183	-5.614	2.385	2.100	4.087
Fe	Al	Al	Al	Si	Al	Si	2.395	3.308	-5.796	1.785	2.423	4.289
Fe	Al	Al	Si	Al	Al	Si	2.421	3.142	-5.645	2.055	1.898	4.109
Fe	Al	Al	Si	Si	Al	Al	2.426	3.272	-5.496	2.837	1.806	3.952
Fe	Al	Si	Al	Al	Al	Si	2.443	3.104	-5.519	2.675	1.444	3.964
Fe	Al	Si	Al	Si	Al	Al	2.419	3.208	-5.515	2.174	1.919	3.963
Fe	Al	Si	Si	Al	Al	Al	2.422	2.744	-5.545	3.146	1.898	4.019
Fe	Si	Al	Al	Al	Al	Si	2.412	3.107	-5.679	1.820	2.071	4.158
Fe	Si	Al	Al	Si	Al	Al	2.423	3.003	-5.613	2.050	1.851	4.072
Fe	Si	Al	Si	Al	Al	Al	2.426	3.229	-5.597	2.474	1.799	4.058
Fe	Si	Si	Al	Al	Al	Al	2.423	3.084	-5.655	1.998	1.866	4.126
Fe	Al	Al	Al	Si	Si	Si	2.418	3.345	-5.723	2.579	1.951	4.198
Fe	Al	Al	Si	Al	Si	Si	2.423	3.207	-5.707	1.910	1.846	4.177
Fe	Al	Al	Si	Si	Si	Al	2.406	3.490	-5.710	2.004	2.195	4.198
Fe	Al	Si	Al	Al	Si	Si	2.424	3.246	-5.654	2.222	1.842	4.126
Fe	Al	Si	Al	Si	Si	Al	2.440	3.326	-5.508	2.642	1.509	3.950
Fe	Al	Si	Si	Al	Si	Al	2.415	3.506	-5.597	1.825	1.998	4.064
Fe	Si	Al	Al	Al	Si	Si	2.415	3.419	-5.663	1.821	2.019	4.138
Fe	Si	Al	Al	Si	Si	Al	2.402	3.480	-5.805	2.502	2.290	4.302
Fe	Si	Al	Si	Al	Si	Al	2.424	3.190	-5.636	1.959	1.828	4.100
Fe	Si	Si	Al	Al	Si	Al	2.419	3.259	-5.726	1.910	1.931	4.199
Fe	Al	Al	Si	Si	Al	Si	2.416	3.341	-5.769	2.116	2.005	4.248
Fe	Al	Si	Al	Si	Al	Si	2.414	3.123	-5.741	1.503	2.036	4.218
Fe	Al	Si	Si	Al	Al	Si	2.391	3.549	-5.866	1.602	2.493	4.371
Fe	Al	Si	Si	Si	Al	Al	2.410	3.330	-5.639	2.014	2.124	4.115
Fe	Si	Al	Al	Si	Al	Si	2.430	3.026	-5.723	1.989	1.723	4.193
Fe	Si	Al	Si	Al	Al	Si	2.406	3.508	-5.907	2.773	2.227	4.421

Fe	Si	Al	Si	Si	Al	Al	2.423	3.130	-5.685	1.869	1.851	4.153
Fe	Si	Si	Al	Al	Al	Si	2.433	3.088	-5.747	2.072	1.665	4.212
Fe	Si	Si	Al	Si	Al	Al	2.454	3.003	-5.618	2.492	1.244	4.071
Fe	Si	Si	Si	Al	Al	Al	2.404	3.474	-5.804	1.774	2.237	4.295
Fe	Al	Al	Si	Si	Si	Si	2.387	3.572	-5.944	1.878	2.610	4.471
Fe	Al	Si	Al	Si	Si	Si	2.387	3.495	-5.856	1.750	2.584	4.362
Fe	Al	Si	Si	Al	Si	Si	2.434	3.303	-5.704	2.604	1.650	4.172
Fe	Al	Si	Si	Si	Si	Al	2.393	3.796	-5.789	2.565	2.460	4.288
Fe	Si	Al	Al	Si	Si	Si	2.424	3.451	-5.655	2.452	1.846	4.132
Fe	Si	Al	Si	Al	Si	Si	2.430	3.256	-5.703	2.695	1.726	4.174
Fe	Si	Al	Si	Si	Si	Al	2.424	3.422	-5.638	2.903	1.843	4.099
Fe	Si	Si	Al	Al	Si	Si	2.409	3.350	-5.828	2.243	2.175	4.334
Fe	Si	Si	Al	Si	Si	Al	2.414	3.363	-5.817	2.116	2.052	4.312
Fe	Si	Si	Si	Al	Si	Al	2.411	3.433	-5.811	2.150	2.107	4.300
Fe	Al	Si	Si	Si	Al	Si	2.407	3.442	-5.826	2.044	2.190	4.319
Fe	Si	Al	Si	Si	Al	Si	2.444	3.088	-5.713	2.708	1.464	4.184
Fe	Si	Si	Al	Si	Al	Si	2.440	3.099	-5.722	2.473	1.523	4.187
Fe	Si	Si	Si	Al	Al	Si	2.434	3.119	-5.849	2.696	1.668	4.342
Fe	Si	Si	Si	Si	Al	Al	2.413	3.351	-5.745	1.921	2.072	4.234
Fe	Al	Si	Si	Si	Si	Si	2.433	3.533	-5.773	3.088	1.688	4.263
Fe	Si	Al	Si	Si	Si	Si	2.408	3.260	-5.886	2.116	2.176	4.387
Fe	Si	Si	Al	Si	Si	Si	2.421	3.187	-5.825	2.344	1.923	4.311
Fe	Si	Si	Si	Al	Si	Si	2.432	3.415	-5.815	3.426	1.732	4.312
Fe	Si	Si	Si	Si	Si	Al	2.408	3.575	-5.807	2.139	2.158	4.299
Fe	Si	Si	Si	Si	Al	Si	2.443	2.985	-5.677	2.343	1.456	4.134
Fe	Si	Si	Si	Si	Si	Si	2.457	3.135	-5.655	3.520	1.221	4.120

Elastic constants of the β-AlFeSi solid solution *end-members* calculated by DFT.

Site							Elastic constants (GPa)												
Fe (1)	Al (1)	Al (2)	Al (3)	Al (4)	Al (5)	Al (6)													
Multiplicity																			
8	8	8	8	8	4	8	C_{11}	C_{12}	C_{13}	C_{16}	C_{22}	C_{23}	C_{26}	C_{33}	C_{36}	C_{44}	C_{45}	C_{55}	C_{66}
Fe	Al	Al	Al	Al	Al	Al	179,0	48,0	58,8	-0,3	178,6	60,0	-0,1	248,6	-0,2	68,7	0,0	79,3	78,8
Fe	Al	Al	Al	Al	Si	Al	184,3	44,6	58,5	-0,3	183,6	59,9	-0,1	281,8	-0,4	68,7	-0,1	83,6	79,9
Fe	Al	Al	Al	Al	Al	Si	217,1	42,7	61,0	-6,3	214,9	62,6	3,1	262,4	-3,2	82,4	3,2	93,5	91,5
Fe	Al	Al	Al	Si	Al	Al	184,7	56,5	61,2	10,3	178,5	60,7	2,9	282,7	-7,5	64,8	6,7	74,8	80,2
Fe	Al	Al	Si	Al	Al	Al	208,1	42,4	64,2	11,4	210,3	65,2	-0,9	250,8	-3,5	76,4	1,8	80,0	76,1
Fe	Al	Si	Al	Al	Al	Al	208,4	42,3	64,0	-11,4	210,3	65,2	0,8	250,7	3,3	76,4	-1,8	80,0	75,9
Fe	Si	Al	Al	Al	Al	Al	217,2	42,7	61,0	6,4	215,0	62,7	-3,0	262,6	3,4	82,4	-3,3	93,6	91,6
Fe	Al	Al	Al	Al	Si	Si	214,4	43,6	64,9	-6,1	213,0	66,1	2,0	281,5	-3,5	75,0	3,5	86,2	87,7
Fe	Al	Al	Al	Si	Si	Al	187,3	56,9	61,4	-12,0	179,1	62,6	-3,7	305,3	7,2	65,8	-7,3	72,9	80,8
Fe	Al	Al	Si	Al	Si	Al	211,0	44,3	65,7	12,1	212,0	67,7	-3,1	270,3	0,2	74,7	3,2	75,0	74,8
Fe	Al	Si	Al	Al	Si	Al	211,3	44,3	65,6	-12,0	212,1	67,8	3,0	270,4	-0,5	74,7	-3,2	75,0	74,7
Fe	Si	Al	Al	Al	Si	Al	214,1	43,7	64,9	6,2	212,9	66,1	-2,0	281,5	3,4	75,0	-3,6	86,1	87,6
Fe	Al	Al	Al	Si	Al	Si	216,2	56,1	67,3	-12,4	208,1	65,2	3,5	284,4	1,6	71,9	5,2	71,0	82,4
Fe	Al	Al	Si	Al	Al	Si	239,0	45,0	64,6	10,2	236,8	67,3	-0,5	250,5	-4,8	81,6	11,1	69,4	83,2
Fe	Al	Al	Si	Si	Al	Al	222,4	43,6	55,2	12,4	201,9	82,0	3,3	261,4	-12,2	74,7	4,3	74,1	89,2
Fe	Al	Si	Al	Al	Al	Si	236,5	44,8	68,4	-19,7	232,8	68,2	7,4	240,7	-4,5	81,4	-1,0	74,1	81,8
Fe	Al	Si	Al	Si	Al	Al	222,8	43,6	54,7	-12,4	201,8	81,9	-3,6	261,6	12,1	74,8	-4,3	74,1	88,9
Fe	Al	Si	Si	Al	Al	Al	178,6	44,2	65,0	-0,8	179,9	64,8	-2,8	237,7	0,5	62,1	-0,5	27,9	45,3
Fe	Si	Al	Al	Al	Al	Si	236,2	49,7	62,8	0,2	239,2	62,2	0,0	255,4	-0,1	83,7	0,1	74,4	73,5
Fe	Si	Al	Al	Si	Al	Al	214,0	52,0	67,5	-0,8	202,9	67,3	-2,6	285,7	7,2	71,0	0,3	80,3	84,7
Fe	Si	Al	Si	Al	Al	Al	235,9	44,9	68,6	19,7	232,8	68,1	-7,5	240,8	4,6	81,4	1,1	74,1	82,0
Fe	Si	Si	Al	Al	Al	Al	239,2	45,0	64,3	-10,2	236,8	67,3	0,3	250,7	4,6	81,8	-11,0	69,3	83,0
Fe	Al	Al	Al	Si	Si	Si	202,9	59,2	72,0	-9,4	197,6	71,5	-1,6	291,9	3,0	64,9	8,9	53,0	71,4
Fe	Al	Al	Si	Al	Si	Si	231,4	49,7	69,7	11,4	225,7	71,7	-4,2	260,8	-3,3	76,3	9,8	45,1	80,0
Fe	Al	Al	Si	Si	Si	Al	204,2	59,2	73,9	0,6	194,3	74,0	-3,8	268,4	5,0	64,4	2,5	41,2	68,7
Fe	Al	Si	Al	Al	Si	Si	231,6	50,4	70,3	-19,8	221,6	67,6	7,4	257,4	-6,6	77,1	-2,1	47,0	80,1
Fe	Al	Si	Al	Si	Si	Al	204,1	59,1	73,9	-0,5	194,2	74,0	3,8	268,2	-5,5	64,5	-2,3	41,1	68,8
Fe	Al	Si	Si	Al	Si	Al	206,9	46,8	82,0	0,3	213,5	82,8	-0,1	229,9	0,0	73,5	0,2	30,9	46,7
Fe	Si	Al	Al	Al	Si	Si	215,0	54,9	70,7	0,3	218,7	69,1	0,0	254,2	-0,3	77,2	0,2	36,2	39,1
Fe	Si	Al	Al	Si	Si	Al	202,6	59,2	72,2	9,7	197,5	71,5	1,6	292,1	-3,5	65,0	-8,7	52,9	71,6

Fe	Si	Al	Si	Al	Si	Al	230,9	50,5	70,4	19,8	221,5	67,4	-7,5	257,4	6,4	77,1	2,4	47,0	80,3
Fe	Si	Si	Al	Al	Si	Al	231,8	49,6	69,5	-11,4	225,8	71,8	4,0	261,0	3,1	76,5	-9,6	45,0	79,9
Fe	Al	Al	Si	Si	Al	Si	227,7	59,6	76,8	-2,1	219,9	73,9	-0,4	245,5	-0,5	74,9	2,4	41,3	72,7
Fe	Al	Si	Al	Si	Al	Si	236,3	55,2	69,7	-14,2	219,0	71,4	7,5	253,8	-5,0	75,9	0,6	52,7	76,7
Fe	Al	Si	Si	Al	Al	Si	230,0	53,4	72,1	-7,0	238,3	70,1	2,9	246,3	-4,0	82,6	3,9	39,0	52,2
Fe	Al	Si	Si	Si	Al	Al	245,8	37,2	75,7	-17,9	249,1	67,5	7,6	220,8	-1,8	85,5	4,7	53,8	79,8
Fe	Si	Al	Al	Si	Al	Si	227,3	65,3	65,9	4,8	223,8	60,4	-3,6	282,0	1,0	83,0	1,1	49,7	64,9
Fe	Si	Al	Si	Al	Al	Si	254,3	54,6	66,0	11,7	247,4	64,5	-3,7	256,0	2,6	89,6	2,2	49,3	77,5
Fe	Si	Al	Si	Si	Al	Al	236,2	55,4	69,9	14,8	219,1	71,3	-7,7	254,4	5,1	76,1	-0,3	53,0	77,0
Fe	Si	Si	Al	Al	Al	Si	254,5	54,5	65,8	-11,3	247,6	64,6	3,8	256,0	-2,6	89,6	-1,9	49,3	77,5
Fe	Si	Si	Al	Si	Al	Al	227,5	59,5	76,8	2,2	219,9	73,9	0,3	245,3	0,4	74,9	-2,1	41,3	72,7
Fe	Si	Si	Si	Al	Al	Al	229,8	53,4	72,2	7,5	238,2	70,0	-3,0	246,5	3,5	82,5	-3,7	38,8	52,2
Fe	Al	Al	Si	Si	Si	Si	217,4	55,3	83,0	-12,2	222,8	81,8	3,5	243,8	-14,8	69,0	4,2	32,8	64,7
Fe	Al	Si	Al	Si	Si	Si	220,6	51,2	76,5	3,1	224,4	73,6	1,9	258,0	5,3	69,8	4,6	42,2	70,9
Fe	Al	Si	Si	Al	Si	Si	225,7	62,4	71,5	-6,5	231,1	71,3	1,2	256,5	-4,1	73,9	5,5	31,1	50,8
Fe	Al	Si	Si	Si	Si	Al	243,0	44,7	77,6	-15,3	246,2	69,9	2,9	224,3	0,6	79,6	4,5	39,0	68,9
Fe	Si	Al	Al	Si	Si	Si	205,4	63,9	83,1	9,0	211,7	72,1	-3,9	239,1	8,1	73,8	-4,4	30,1	56,0
Fe	Si	Al	Si	Al	Si	Si	242,7	53,7	67,5	9,8	236,6	67,6	-0,2	257,5	10,2	87,0	0,7	43,8	60,4
Fe	Si	Al	Si	Si	Si	Al	220,7	51,2	76,6	-2,9	224,5	73,6	-1,9	257,7	-5,4	69,8	-4,3	42,1	71,1
Fe	Si	Si	Al	Al	Si	Si	242,9	53,8	67,6	-9,2	236,4	67,7	0,0	257,5	-10,4	87,0	-0,4	43,7	60,3
Fe	Si	Si	Al	Si	Si	Al	217,2	55,4	82,9	12,3	222,8	81,7	-3,7	244,2	14,7	69,1	-3,9	32,8	64,7
Fe	Si	Si	Si	Al	Si	Al	225,5	62,4	71,6	7,0	231,1	71,2	-1,1	256,5	3,7	73,9	-5,2	31,0	50,9
Fe	Al	Si	Si	Si	Al	Si	253,0	47,1	72,9	-12,3	261,2	64,9	3,9	241,8	-7,6	86,0	8,2	43,9	82,4
Fe	Si	Al	Si	Si	Al	Si	252,8	49,5	71,9	-9,0	265,9	69,3	0,8	237,4	-14,1	91,8	-4,4	41,3	77,3
Fe	Si	Si	Al	Si	Al	Si	252,6	49,5	71,6	9,3	266,0	69,3	-0,9	237,9	14,0	91,7	4,7	41,3	77,2
Fe	Si	Si	Si	Al	Al	Si	250,9	59,3	71,3	3,9	254,3	68,3	-4,1	252,7	10,3	92,0	1,1	45,9	62,5
Fe	Si	Si	Si	Si	Al	Al	245,7	44,2	71,4	-2,3	251,5	71,7	3,0	241,8	-7,8	87,4	-2,6	44,7	79,5
Fe	Al	Si	Si	Si	Si	Si	255,9	51,2	70,9	-11,0	265,6	68,4	-0,1	241,9	-3,0	81,4	10,3	45,7	77,5
Fe	Si	Al	Si	Si	Si	Si	251,0	46,8	70,9	-8,8	257,5	72,1	-5,6	247,5	-7,0	89,0	-4,5	55,4	77,1
Fe	Si	Si	Al	Si	Si	Si	250,7	46,7	70,9	9,1	257,5	72,2	5,6	247,7	6,9	88,8	4,8	55,4	77,0
Fe	Si	Si	Si	Al	Si	Si	237,6	63,5	71,1	0,6	244,2	67,7	1,4	257,4	4,6	83,4	-1,9	42,2	52,4
Fe	Si	Si	Si	Si	Si	Al	237,4	51,9	73,0	-2,0	246,4	72,9	1,8	249,1	-5,2	81,5	-2,0	41,3	72,1
Fe	Si	Si	Si	Si	Al	Si	258,1	45,3	74,0	-3,9	261,1	80,7	-3,9	222,8	-5,7	99,3	3,5	65,9	82,5
Fe	Si	Si	Si	Si	Si	Si	248,4	47,8	70,5	-3,0	249,7	82,6	-8,7	246,9	-0,7	92,8	0,9	68,2	66,0

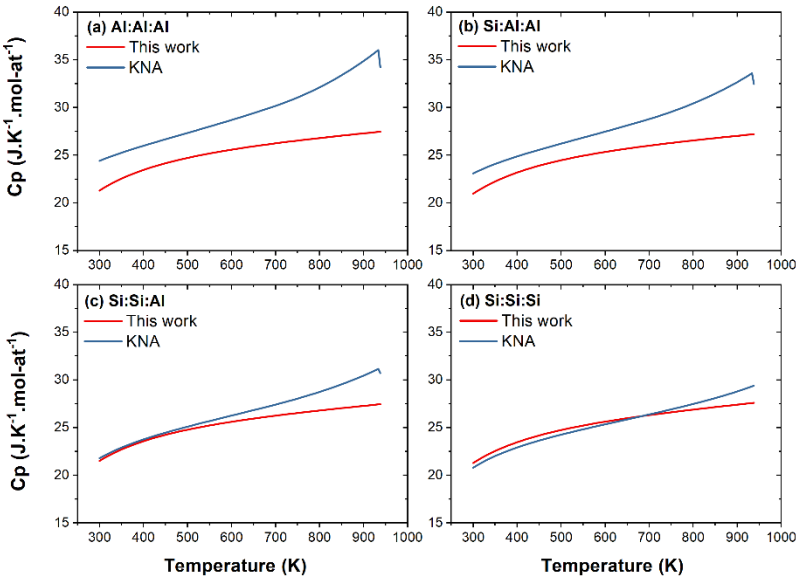

Heat capacity calculation of the stable 3-SL end-members of the β-AlFeSi solid solution compared to the heat capacity derived from the Kopp-Neumann Approximation (KNA)